Protonium and baryonium states with the Graz potential

Rubin H. Landau and J. Schnick
Physics Department, Oregon State University, Corvallis, Oregon 97331
(Received 11 June 1987)

Atomic and nuclear complex energy (Gamow) states of the $\bar{p}p$ system are calculated with the Graz potential. The Coulomb force is included exactly (numerically), separate channels and experimental masses are used for $\bar{p}p$ and $\bar{n}n$, and absorption is included via a phenomenological annihilation channel. Significant model dependence of the $n=1$ $^1S_0$ protonium level is found, as is a possible systematic difference among most calculations and recent experiments. Bound and resonant states of baryonium are found in a number of charge and isospin channels, some with widths as narrow as 16 MeV. Unphysical zero width states are also found and analyzed.

I. INTRODUCTION

The proton p and the antiproton $\bar{p}$, having opposite quantum numbers and charge, can form bound states. Yet bound states with quantum numbers of zero can spontaneously annihilate into the vacuum and these states are all unstable. When most of the binding arises from Coulomb attraction the states are those of an exotic atom of Bohr radius 58 fm and binding energy 12.5 keV, known as "antiprotonic hydrogen" or "protonium." When most of the binding arises from nuclear attraction, the states are those of an exotic nucleus of radius 1–2 fm and binding energy in MeV's, known as "baryonium." Knowledge about both kinds of states is limited since they do not occur naturally; there have been few $\bar{p}$ facilities to study them, and they annihilate rapidly.

The unequivocal observation of low-lying protonium states is a challenge to the experimental art only now yielding to the intensity of the Low Energy Antiproton Ring at CERN. Although annihilation causes the yields to be too low to observe a full cascade of x rays down to the $n=2$ or 1 protonium shells, it is rather certain that the individual L lines at 1.71 keV (Ref. 1) and the K lines at 9.4 keV (Refs. 2–4) have been seen. Studying this exotic atom is more than a technical challenge, it is a good way to learn about the largely unknown $\bar{p}p$ strong interaction. Specifically, the observed shift of the atomic levels *upwards* to less bound energies—in spite of the exceptionally strong attraction of the $\bar{p}p$ nuclear force—can be caused by the presence of baryonium levels far below the atomic ones, or by very strong absorption.[5] Indeed, some researchers have concluded that there must be baryonium present[6] since the shifts are so large.

The existence of baryonium states is controversial since the $\bar{p}p$ potential—or even the limits to a potential description of particle-antiparticle interactions—is not well understood. It is known that taking the G-parity transformation of the meson-theoretic, nucleon-nucleon (NN) potential yields an $\bar{N}N$ potential with significantly greater attraction (≈ 2 GeV) than the NN one. Consequently, since the NN potential is strong enough to support a single strong bound state, the deuteron, the more attractive $\bar{N}N$ potential should be able to support even more. Indeed, many works,[7–12] possibly beginning with that of Shapiro,[13] have found many states of baryonium.

The problem in the preceding logic is that the meson-theoretic potentials are—at best—valid only at medium and large distances, and they fail to describe the short ranged (≤ 0.2 fm), and important, annihilation. Calculations including annihilation sometimes find that it either eliminates the bound states,[14] or gives them such large widths as to make them barely, if at all, observable.[9,11,15]

Since annihilation is a multiparticle, short ranged, and high energy process, elementary quark degrees of freedom within the baryons may be excited, and it is not surprising that much attention is being paid to describing annihilation with quantum chromdynamics (QCD), or quark bag models of QCD.[11,15,16] In fact, if baryonium is an elementary two-quark–two-antiquark state $(2q,2\bar{q})$, then it is formed after a $q\bar{q}$ annihilation, and the potential approach [which models it is as a $\bar{N}N$, i.e., a $(3q,3\bar{q})$ state] may be doomed to failure. Likewise, if baryonium is a $(2q,2\bar{q})$ state, it would be a doorway for the annihilation process, and a meson approach to annihilation (i.e., the rearrangement of six quarks without annihilation) may also fail.

Even if the $\bar{N}N$ potential exists and is known, the type of calculation presented in this paper, an accurate determination of the $\bar{N}N$ atomic and nuclear eigenenergies, is also an active research problem. Inasmuch as these states decay in time, they are not conventional bound states and their calculation requires quantum mechanics to be extended to complex energies (whether the energy is complex because the potential is complex or because there is an explicit coupled channel is not crucial; in either case we are trying to model a many-body, coupled-channels, time-dependent phenomenon with a time-independent, one-body Schrödinger equation). Sometimes these states are called "unstable" bound states, sometimes Gamow or resonant states,[17–19] sometimes quasistationary states, and sometimes complex-energy states. *Regardless of the name,* many of the usual prescriptions regarding normalizations, orthogonality, eigenvalues, and Green's functions need reinterpretation for both the single channel,[20] and for coupled-channels[21,22] cases.

While the possibility of directly observing narrow, baryonium states is still raised,[7,11] the signature is uncertain; e.g., they can also be interpreted as unusual, meson-meson resonances. In contrast, protonium states have a clear experimental signature, and the widths and shifts (from pure Coulomb energies) of their levels are a direct measure of the nuclear interaction—and possibly of the existence of baryonium. We study both protonium and baryonium with the view that a serious study of the protonium states is required before baryonium states can be predicted.

Recently, the group at Graz, Schweiger, Haidenbauer, and Plessas[23] (SHP), produced a semimicroscopic $\bar{\text{N}}$N potential. It is a multiterm, nonlocal, separable interaction, appropriate to a Schrödinger equation with separate coupled channels for $\bar{\text{p}}$p, $\bar{\text{n}}$n, and annihilation (more details are given in the theory section). Insofar as the Graz potential has a good theoretical pedigree, a realistic description of channel coupling, and an excellent fit to scattering data, it promises to have realistic and engaging bound state properties; we study them and report the results here. The nonlocality and channel coupling of this potential require some nontraditional techniques to solve for its combined Coulomb plus nuclear bound states. These techniques are now available with the momentum space codes BOPIT (Ref. 20) and LPOTBS,[21,22,24] and we make the first application of the latter code (which can handle coupled channels) to antiprotons.

The original motivation for our calculation was to test these rather new theoretical tools on antiprotons and compare the results obtained with the Graz potential to those obtained by other researchers[8,11,15,25] using different potentials and different calculational techniques. (This approach was helpful in the analogous K$^-$p problems[22,24,26] where it led to improvements in the technique,[22,24] suggested a reinterpretation of experiments,[26] and led to the development of the new $\bar{\text{K}}$N potential.[27]) In the course of our study, its timeliness was heightened by the appearance of experimental results on protonium.[1,2,3,4] While the experimental results appear to be converging there are still large uncertainties. Seeing that the Graz potential is probably the best of the potential models available, and it is still uncertain whether a potential model can be successful, broad comparisons of this model with other models and all data are given.

II. THEORY

A. Evaluation of the Graz potential

The Graz potential[23] originates from the Paris, meson-theoretic NN potential[9,28] G parity transformed to obtain the elastic (real) part of the $\bar{\text{N}}$N potential. The inner region ($r < 0.8$ fm) is set to zero and annihilation is included by coupling the nucleon (N) channels to two boson (B) channels for each isospin:

$$|\bar{\text{N}}\text{N},I=1\rangle,\quad |\bar{B}B,I=1\rangle\,,$$
$$|\bar{\text{N}}\text{N},I=0\rangle,\quad |\bar{B}B,I=0\rangle\,. \tag{1}$$

With no interaction within the annihilation (A) channels, $T(\bar{B}B\to\bar{B}B)=V(\bar{B}B\to\bar{B}B)=0$, the coupling to these channels is equivalent to an energy-dependent potential in the elastic channels:

$$V^I_{\text{ann},LL'}=V^{I\dagger}_{A,JL}(E-\Delta m_{1A}-h^I_{0,J}+i\varepsilon)^{-1}V^I_{A,JL'} \qquad (I=0,1)\,. \tag{2}$$

Here h^I_0 denotes the free Hamiltonian in the annihilation channels, $\{L,L',J\}$ are angular-momentum labels, and Δm_{1A} is the annihilation-channel threshold energy (chosen to be -300 MeV, i.e., $m_B=788$ MeV, an average value for ρ and ω).[29]

To include the neutron-proton mass splitting and the Coulomb force, SHP transform to the charge basis,

$$|1\rangle=|\bar{\text{p}}\text{p}\rangle,\quad |2\rangle=|\bar{\text{n}}\text{n}\rangle\,, \tag{3}$$

$$V_{11}=V_{22}=\tfrac{1}{2}(V^0+V^1),\quad V_{12}=V_{21}=\tfrac{1}{2}(V^0-V^1)\,, \tag{4}$$

and fit all available elastic, charge exchange, and annihilation cross section data below 150 MeV for ($L\le 2$, $J\le 3$). Their final result is a nuclear potential containing strong and annihilation parts, each part fit to multiterm separable potentials:

$$V_{\text{nucl},LL'}=V_{\text{ann},LL'}+V_{s,LL'}\,, \tag{5}$$

$$V_{s,LL'}=\sum_{i,j=1}^{N}|g_{Li}\rangle\lambda_{ij}\langle g_{L'j}|\,, \tag{6}$$

$$V_{A,JL}=|g^a_J\rangle\kappa_{JL}\langle g^a_L|\,, \tag{7}$$

with each $g_n(\text{p})$ the ratio of polynomials. In this notation, the $\bar{\text{N}}$N pair is in a state with coupled, orbital angular momenta $(L',L)=(L_>,L_<)$, and total angular momentum J. The $\bar{B}B$ pair into which $\bar{\text{N}}$N annihilate is spinless and so must have total (now equal to orbital) angular momentum J; e.g., the $^1S_0$ fermions couple to the $^1S_0$ bosons, yet the $^3S_1$ fermions couple to $^1P_1$ bosons (as do $^3D_1$ fermions).

Inasmuch as SHP do not give directly calculable expressions for their potentials, we provide some details here. We follow their notation except for a slight difference in normalization:[21,22]

$$\langle\mathbf{p}|V|\mathbf{p}'\rangle=\int d^3r\,d^3r'\frac{e^{-i\mathbf{p}\cdot\mathbf{r}}}{(2\pi)^{3/2}}\langle\mathbf{r}|V|\mathbf{r}'\rangle\frac{e^{i\mathbf{p}'\cdot\mathbf{r}'}}{(2\pi)^{3/2}}$$
$$=\frac{1}{2\pi^2}\sum_{L=0}^{\infty}(2L+1)V_L(\text{p},\text{p}')P_L(\cos\theta)$$
$$=\tfrac{1}{2}\pi V^{\text{Graz}}\,. \tag{8}$$

An explicit evaluation of (2) yields:

$$V_{\text{ann},LL'}(k,k')=\tfrac{1}{2}\pi\kappa^a_{JL}\kappa^a_{JL'}g^a_L(k)g^a_{L'}(k')m_BI_J(E)\,, \tag{9}$$

$$I_J(E)=\int_0^\infty dp\,p^2\frac{g^a_J(p)^2}{m_B(E-\Delta m_{1A}-p^2/m_B+i\varepsilon)}\,. \tag{10}$$

Although it is possible to evaluate $I_J(E)$ analytically (presumably what SHP do), we use numerical integration and check it against the analytic expression (we get eight-place precision for 32 Gauss points). For real energy E

$$I_J(E)=\int_0^\infty dp\, p^2 \frac{g_J^a(p)^2}{k_A^2-p^2+i\varepsilon}$$
$$=\int_0^\infty dp\, p^2 \frac{g_J^a(p)^2}{(k_A-p+i0)(k_A+p)} , \quad (11)$$

where we have introduced k_A, the on-shell momentum in the annihilation channel:[29]

$$k_A=\pm\sqrt{m_B(E-\Delta m_{1A})}=\pm\sqrt{m_B(E+300\text{ MeV})} . \quad (12)$$

If $E<\Delta m_{1A}$, the annihilation channel is closed, there is no zero possible in the denominator in (10), the $i\varepsilon$ prescription can be ignored, and V_{ann} is real. If $E>\Delta m_{1A}$, the channel is open, we take the positive square root for k_A and separate I_J into delta function and principal value parts:

$$I_J(E)=-\tfrac{1}{2}i\pi k_A g_J^a(k_A)^2+\mathrm{P}\int_0^\infty dp\, p^2 \frac{g_J^a(p)^2}{k_A[E]^2-p^2} . \quad (13)$$

The annihilation channel manifestly produces a complex and energy-dependent potential. The principal part integral is evaluated numerically with the Haftel-Tabakin[30] procedure:

$$I_J(E)=-\tfrac{1}{2}i\pi k_A g_J^a(k_A)^2 + \int_0^\infty dp \frac{[p^2 g_J^a(p)^2-k_A^2 g_J^a(k_A)^2]}{k_A^2-p^2} . \quad (14)$$

To search for complex eigenenergy, baryonium states, we must analytically continue the Graz potential to complex energy. Whereas the potential (and the Green's functions of subsection B) depend on momentum, we must also continue into the complex momentum plane. Given a complex momentum k_R+ik_I it is easy to determine the complex energy as

$$E_R+iE_I=(k_R^2-k_I^2+2ik_R k_I)/2m \quad (15)$$

[but note that the inverse, e.g., (12), has ambiguities]. Seeing that normal bound states of negative, pure real energy occur on the positive imaginary axis $k_0=+i\kappa$, we continue them into the second quadrant of the complex k plane in order to produce decaying states with a negative E_I. Resonances, normally occurring right below the real positive energy axis, continue into the fourth quadrant of the complex k plane and are also decaying states.

The basic definition of I_J (10) can be evaluated directly (numerically) for complex energies—yet not for the important case of E approaching the positive real axis from above. We analytically continue (14) to complex energies with the following prescription for k_A: If $k_A^2>0$, the annihilation channel is open and the two bosons are in a resonancelike state; we therefore choose the sign in (12) which gives k_A a positive real part. If $k_A^2<0$ ($E<-300$ MeV), the annihilation channel is closed and the two bosons are in a boundlike state; we therefore choose the sign in (12) which gives k_A a positive imaginary part. We thus exclude the possibilities of the $\bar{B}B$ system being a negative energy virtual bound state ($\mathrm{Im}k_A<0$), or a positive energy bound state ($\mathrm{Im}k_A>0$); these poles of the T matrix are of less experimental consequence.

Although (14) looks like the separation of the Green's function into delta function and principal value parts, that is true only for real E's. For complex E, the first term is that obtained from Cauchy's theorem being applied to the pole of the Green's function (denominator) in (10), while the subtraction in the second term (there to implement the principal value subtraction for real energies) eliminates double counting the pole contribution. The apparent imaginary part turns real as the annihilation channel closes and $k_A\to+i\kappa$.

B. Complex energy states for coupled channels

We solve the Coulomb plus nuclear problem exactly (in a numerical sense) for protonium and baryonium states (be they Gamow, resonant, unstable bound, etc.) by extending the momentum space code LPOTBS (Refs. 21 and 22) to permit searches in all four quadrants of the complex momentum plane. This technique looks for solutions of the Lippman-Schwinger equation (without the homogeneous, or plane wave, solution)

$$\begin{bmatrix} T_{11} & T_{12} \\ T_{21} & T_{22} \end{bmatrix} = \begin{bmatrix} V_{11}G_1 & V_{12}G_2 \\ V_{21}G_1 & V_{22}G_2 \end{bmatrix} \begin{bmatrix} T_{11} & T_{12} \\ T_{21} & T_{22} \end{bmatrix} , \quad (16)$$

where G_i is the free Green's function for channel i. The requirement of a nontrivial solution to (16) reduces to a search in the complex energy plane for the zeros of the determinant:

$$\det[1-V(E)G(E)]=0 . \quad (17)$$

This is the same condition as searching for the poles of the coupled channels T matrix $T=(1-VG)^{-1}V$, with the poles arising from the denominator, not the numerator. (The poles of the numerator V are the "potential" or "fixed" poles and are of less appeal since they are sensitive to details of the potential model and not particle dynamics.)

The momentum space equivalent of choosing boundary conditions in coordinate space is specifying Green's functions and their singularities. For real energies,[31] we take the Green's function for channel i as:

$$\langle p\,|\,G_i\,|\,p\rangle=(E+\Delta M_{1i}+i\varepsilon-p^2/2\mu_i)^{-1} , \quad (18a)$$
$$=P(E+\Delta M_{1i}-p^2/2\mu_i)^{-1} - i\pi\delta(E+\Delta M_{1i}-p^2/2\mu_i) , \quad (18b)$$

with μ_i the reduced mass in channel i, and ΔM_{1i} the difference in total mass from channel 1. If channel i is open (i.e., we are at positive energies), the delta function part of (18b) contributes an imaginary part to G, and the "eigenenergies" satisfying (18) will be complex numbers—even if all potentials are real. As discussed in the preceding section, the generalization of (17) for complex energies will be of the same form, with the delta function part continuing into the pole term contribution and the principal part integral containing a subtraction of the pole term.

The momentum-space Coulomb force is included with the Kwon, Tabakin, and Landé procedure[17,21] in which the Coulomb part of V_{11} contains an exact "correction term" along the diagonal to remove the singularity at $k'=k$. For example, when the integrals are replaced by sums over N grid points p_m and weights W_m, the nondiagonal potential is proportional to the second kind of Legendre function (the one singular at $k=k'$):

$$V_{c,L}(k,k')=-\frac{Ze^2}{2kk'}Q_L(z_{kk'}) ,\quad z_{kk'}=\frac{k'^2+k^2}{2k'k} . \tag{19}$$

The diagonal part of the Coulomb potential now contains the "correction" to remove the contribution from the $p_m=p_n$ singularity:

$$V_{c,L}(p_m,p_m)=\left[\int_0^\infty dp'\frac{V_{c,L}(p_m,p')}{P_L(z_{p_mp'})} - \sum_{n\neq m}^{N} W_n\frac{V_{c,L}(p_m,p_n)}{P_L(z_{mn})}\right]\Big/ W_m . \tag{20}$$

The equation we actually solve is the matrix form of (17),

$$\det\begin{bmatrix}\delta_{mn}+V_L^{11}(p_m,p_n)D_1(p_n) & V_L^{12}(p_m,p_n)D_2(p_n)\\ V_L^{21}(p_m,p_n)D_1(p_n) & \delta_{mn}+V_L^{22}(p_m,p_n)D_2(p_n)\end{bmatrix}=0 , \tag{21}$$

where D_i are weighted Green's functions.

III. RESULTS

A. Protonium states

Exact solutions for the complex-eigenenergies states of protonium are given in Table I and Fig. 1 for angular momentum $^{2S+1}L_J={}^1S_0$, and in Table III for $^1P_1$. The results for principal quantum numbers $n=1,2,3$ are presented as ΔE, the complex energy shift from the nonrelativistic, point Coulomb (Bohr) energies, and as the conventional atomic shift and width (ε,Γ):

$$\Delta E=(E_R+iE_I)-E_{\text{Bohr}} ,\quad \varepsilon=E_{\text{Bohr}}-E_R ,\quad \Gamma=-2E_I=-2\Delta E_I . \tag{22}$$

Use of a relativistic wave equation changes the pure Coulomb energies by 1 eV or less, a number much smaller than other theoretical and experimental uncertainties. In contrast, use of a relativistic Schrödinger equation for the *combined* Coulomb plus nuclear forces changes the atomic shifts by several percent (10 eV) and the nuclear levels by 10% or more, yet we tabulate results only for nonrelativistic calculations—to be consistent with the Graz potential's derivation and to permit comparison with the work of others. We also do not tabulate corrections due to the finite size of the Coulomb potential—which we estimate to be as large as 5 eV for the 1 S state.[32]

1. Comparison of calculations

Four potentials are compared in Tables I–III, and Fig. 1: (1) the Graz potential, used by Schweiger *et al.*[23] and the present work (heavy solid and dotted lines), which is nonlocal, energy dependent, and couples several channels in momentum space; (2) the Dover-Richard-1 (DR1) potential,[10] used by Richard and Saino[25] (dashed line) which is local, single channel, complex, and also derived in part from the Paris NN potential,[9] (3) the Green and Wycech[11] potential, which is separable with Gaussian form factors (dot-dashed line); (4) the Bryan-Phillips potential, modified by Alberg *et al.*[15] to include short range behavior and annihilation motivated by quark bag models (solid line).

Considering that the detailed calculational methods differ in all cases, a truly precise comparison of just the different potentials may not be possible, yet a comparison of the three "exact" methods should be valid. We find that in spite of the diverse methods of calculation and different models for annihilation, most of the predicted complex shifts are rather similar (within 13% for ε and 25% for Γ); in particular the Graz (heavy solid line) and DR1 (dashed line) potentials produce similar results. In contrast, the Geo8 potential of the Washington group (solid curve) predicts a complex shift significantly larger in magnitude (actually they published some 16 different shifts, we present their lowest χ^2 fit).

Three calculational methods are compared in Tables I and III: (1) The Trueman approximation[33] that the complex energy shift of an atomic level with Coulomb energy E_n and Bohr radius R_B, is proportional to the complex, strong interaction scattering length "a":

$$\frac{\Delta E_n}{E_n}\approx-\frac{4a}{nR_B} , \tag{23}$$

or more sophisticated versions in which Coulomb and recoil effects are included.[11] (We have extended the Scheiger *et al.*[23] and Green and Wycech[11] results in or-

TABLE I. Complex energy shift of $^1S_0$ protonium level calculated by Refs. 23 (Graz), 25 (Richard and Siano, RS), 11 (Green and Wycech (GW), 15 (Wilets, W), and the present work (RHL). Potentials from Refs. 23 (Graz) and 10 (DR1).

Who	Method	Potential	$\Delta E_{n=1}$ (eV)	$\Delta E_{n=2}$ (eV)	$\Delta E_{n=3}$ (eV)
Graz	$\Delta E\alpha a$	Graz	$600-i570$	$75-i71$	$22-i21$
GW	$\Delta E\alpha a$	own	$590-i660$	$74-i83$	$22-i24$
RHL	exact (**p**)	Graz	$519-i444$	$64-i57$	$17-i17$
RS	exact (**r**)	DR1	$540-i510$	$68-i66$	$20-i20$
W	exact (**r**)	Geo8	$842-i867$		

der to make Table I more complete.) (2) The "exact (**r**)" method of Refs. 25 and 15 is a solution of the single channel, **r**-space Schrödinger equation for the eigenenergies of a local, complex potential. (3) The "exact (**p**)" method described in Sec. II B is a search for the complex-energy poles of a T matrix arising from the Coulomb plus nonlocal, coupled channels, nuclear potential.

As indicated above, the similarity of our results with those of Richard and Saino[25] is at least a partial confirmation of the recently developed "exact (**p**)" method. As seen by comparing the dotted and heavy solid lines in Fig. 1, the Trueman formula Eq. (23) is found not to be good for quantitative study of this strongly absorptive system in the $n=1$ $^1S_0$ state (the $\approx 15\%$ error is comparable to that found for kaons,[22,24] yet much larger than for pions). Inasmuch as this is an on-energy-shell approximation, its lack of accuracy is consistent with there being off-shell sensitivity in these states. We have found, however, that the interaction in the $n=2,3$ states is weak enough for the exact calculations to at least scale in accord with Eq. (23).

We have also investigated P states. Unfortunately, our numerical error for the P state ε is comparable to ε (we calculate an energy of the $\bar{p}p$ system of ~ 3 keV, and subtract the Coulomb energy to obtain a shift of only ~ 4 meV). However, since no subtraction is required for the widths, there is no cancellation; we present results in Table III for the $n=2$ and $n=3$ shell $^1P_1$ widths. The agreement with Richard and Saino[25] is surprisingly good considering that we have used different models for the annihilation and very different calculational techniques. Apparently, the interaction is not strong enough in these P states to drive the $\bar{p}p$ far off its energy shell. All calculations agree with the experimental lower limit of Gorringe *et al.*[2]

TABLE II. Complex energy shift of the $^1S_0$ protonium level measured by Refs. 4 (*), 2 (PLG), and 3 (PS174).

Experiment	Method	$\Delta E_{n=1}$ (eV)
*	XDC	500 ± 300
PLG	Si(Li)	$730-i425$
PS174	*GSPC*	$800-i(\leq 475)$
PS174	Si(Li)	$760-i265$

2. Comparison with experiments

The results of experiments are given in Table II and shown in Fig. 1. The experiments of Gorringe *et al.*,[2] the gas and solid state counter measurements of Baker *et al.*,[3] and the ASTERIX collaboration[4] all agree—within the large error bars. Whereas large systematic errors are a concern since only uncorrelated gamma rays are observed, the overlap of the results supports the belief that the $1S$ state has—at least— been observed. Unfortunately, such large experimental uncertainties do not provide a demanding test of theory.

The general trend evident in Fig. 1 is the agreement among all models, methods, and experiments that the $n=1,2,3$ $^1S_0$ protonium levels are shifted upwards (i.e., less bound than pure Coulomb levels). Whereas the attractive nuclear potential would normally be expected to increase the binding of these atoms, the decrease may indicate nuclear states at a lower energy, i.e., baryonium, or very strong absorption—both effects studied in the analogous $\bar{K}N$ problem.[5,21,22]

Although firm conclusions are difficult to draw with the experiments and calculations in such early stages, there does appear to be large, possibly systematic, disagreement between the experimental points and the exact calculations (dotted and solid lines). Seeing that the potential models all reproduce the scattering data (albeit to differing degrees), the differences with experiment probably reflect the nuclear interaction in the $n=1$, $^1S_0$ state being strong enough to force the $\bar{p}p$ system significantly far off its energy shell. That is, while the scattering experiments used to determine the potentials probe only the asymptotic part of the $\bar{p}p$ wave func-

TABLE III. Width of the $^1P_1$ protonium level with principal quantum number 2,3 calculated by Ref. 25 (Richard and Siano, RS) and the present work (RHL). Potentials from Refs. 23 (Graz) and 10 (DR1); experiment is Ref. 2.

Who	Method	Potential	$\frac{1}{2}\Gamma$ (MeV) $n=2$	$\frac{1}{2}\Gamma$ (MeV) $n=3$
RHL	exact (**p**)	Graz	12	4.3(0.1)
RS	exact (**r**)	DR1	13	4.4
Graz	$\Delta E\alpha a$	Graz	13	3.9
PLG	expt	Si(Li)	≥ 7	

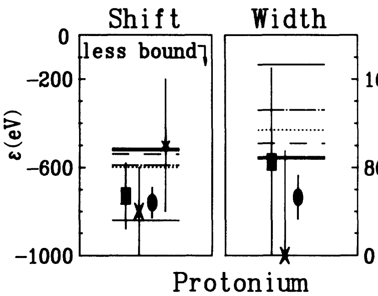

FIG. 1. Shift and width of the $n=1$ $^1S_0$ protonium level as measured by Refs. 4 (star), 2 (box), and 3 (oval, solid state detector; ×, gas detector). The "×" point for Γ is a lower limit. The theoretical lines are as follows: heavy solid—Graz potential, exact (p); dotted curve—Graz potential, Trueman formula; dashed curve—Dover/Richard potential, exact (r), Ref. 25; dot-dashed curve—Green/Wycech potential approximate, Ref. 11; and solid curve—Washington potential, exact (r), Ref. 15.

tion (outside of the interaction region), these atomic experiments apparently probe it at much shorter distances. Alternatively, disagreement between theory and experiment may mean that a potential model cannot provide an accurate enough description of annihilation to produce agreement within the precision of atomic experiments.

B. Baryonium states

We identify solutions of Eq. (19) with Bohr-type energies as protonium. We identify solutions with much larger energies as levels of baryonium. A somewhat unique aspect of our study is its search for states of the experimentally-accessible, p̄p system coupled to n̄n. As seen in Tables IV and V and Fig. 2, we find bound and resonant baryonium charge states and similar states in one or both isospin channels. This is different from our study of the K^-p system,[21,27] where the strong bound states occur only in definite isospin channels.

A traditional technique for finding states coupled strongly to absorption channels is to "turn off" the absorptive parts of the potential, find the zero width states, and then follow these states in the complex plane as the absorption is gradually increased. A typical result of

TABLE IV. Bound and resonant states of p̄p baryonium.

$E(^1S_0)$ (MeV)	$E(^1P_1)$ (MeV)	$E(^3P_0)$ (MeV)
$-356-i0$	$-266-i16$	$-302-i0$
	$-205-i115$	
$28-i9$	$74-i23$	$185-i141$
$77-i32$	$80-i12$	
$181-i42$	$141-i47$	
$435-i65$	$167-i48$	

TABLE V. (Upper) Bound and resonant baryonium states of the $I=0$ $\bar{N}N$ system. Lower: Bound and resonant baryonium states of the $I=1$ $\bar{N}N$ system.

$E(^1S_0)$ (MeV)	$E(^1P_1)$ (MeV)	$E(^3P_0)$ (MeV)
$-354-i0$	$-266-i16$	$-302-i0$
$37-i6$	$31-i1$	$34-i7$
$76-i32$	$79-i12$	$77-i6$
$181-i42$	$166-i48$	$185-i141$
$401-i64$		$237-i3$
$729-i67$		
$-364-i0$	$-205-i116$	
$28-i9$	$73-i23$	$33-i1$
$66-i15$	$343-i58$	$83-i2$
$189-i24$		$182-i2$
$435-i65$		$367-i1$

this procedure for the $^1S_0$ Graz potential is seen in Fig. 3; we see the $V_{\text{ann}}=0$ bound states at -20 and -18 MeV develop widths, move to the continuum, and terminate at $(77,-i32)$ and $(28,-i19)$ MeV. Additional states in the continuum are found and are listed in Table IV for the p̄p charge basis, and in Table V for the isospin basis. Each charge-basis state is seen to have an analogous isospin-basis state.

The particular allure in baryonium states is to find some with narrow widths since these would have longer lifetimes, be easier to observe, and may be of dynamical significance. Indeed, we can see in Tables IV and V, negative energy bound states with (nonzero) widths as small as 16 MeV and as large as 115 MeV. These are important results of this study since they may be experimentally accessible.

A startling result of our search, evident in Tables III and IV, is the existence of deeply bound ($|E_R|\geq 300$ MeV) states with widths equal to 0 (within our numerical precision of 1:10^4). To understand these states, in Fig. 4 we show $E_R(^1S_0)$ as a function of the strength of the annihilation potential. The movement of these poles indicates that the deeply bound states are not "fixed" potential singularities related to the particular potential shape studied. The increasing binding energy and decreasing width found with increasing absorption is rem-

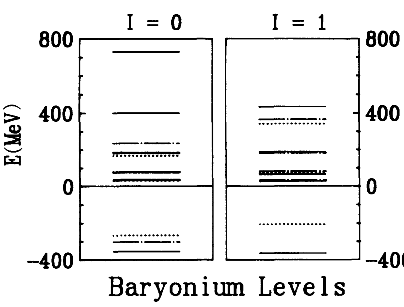

FIG. 2. Bound states and resonances of the Graz potential in the isospin basis: solid—$^1S_0$, dot-dashed—$^3P_0$, dotted—$^1P_1$.

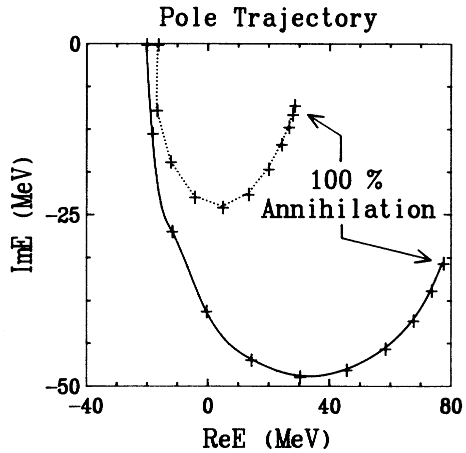

FIG. 3. Trajectories in the complex energy plane of two baryonium levels. Starting at negative E_R, each + represents a 10% increase in annihilation strength.

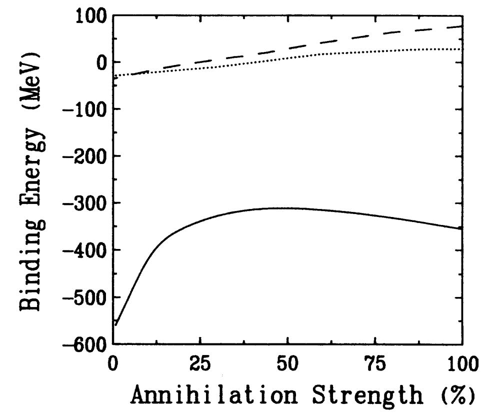

FIG. 4. Baryonium binding energy as a function of annihilation strength. The lower state is below the annihilation threshold energy and thus has zero width. The upper dotted (dashed) curve corresponds to the dotted (solid) curves in Fig. 3.

iniscent of the Krell-Seki oscillations found in $\bar{K}$ nucleus[5] and $\bar{K}N$ (Ref. 21) studies of strongly absorptive potentials. Yet these states are even more unusual in that they disappear when the coupling is not large enough to produce binding energy of at least 300 MeV, the threshold energy Δm_{1A} for the annihilation channel in the Graz potential.[23] That is, for energies 300 MeV below the elastic threshold, the annihilation channel closes and its contribution to the potential (9) and (10) becomes pure real. These deep, stable states may be fascinating, but are artifacts of this particular model: If the threshold had been placed at $2m_\pi$ rather than 2 (788 MeV), these states would acquire a width.[29]

IV. SUMMARY AND CONCLUSIONS

We have applied momentum-space techniques to study the bound and resonant states of protonium and baryonium. By providing an exact solution of the Coulomb plus nuclear-force problem, even for coupled channels, comparison among various theories as well as with experiments can be made without questions regarding technique.

The input to our $\bar{p}p$ study is the modern and realistic, Graz $\bar{N}N$ potential model.[23] This potential fits most low energy scattering and reaction data, has separate channels for $\bar{n}n$, $\bar{p}p$, and annihilation, originates from the Paris meson-theoretic NN potential, and is nonlocal and energy dependent.

Our calculation of the states of protonium appear consistent with other published calculations yet does show significant model dependence for the $n=1$ $^1S_0$ state. As also found for antikaons, the Trueman formula[33] is not accurate enough for quantitative study; in the antikaon case because of nearby open channels, in the present case because of off-shell effects.

Even with the present early state of theory and experiment, there may be large, possibly systematic, differences among most calculations and the several recent protonium measurements.[1-4] Whether this reflects a hoped-for sensitivity of the level shifts to the short range part of the $\bar{N}N$ interaction (off-energy-shell effects), or a breakdown of the microscopic potential approach is now an important, open question. Better theory and experiment is called for, as are analogous studies of the $\bar{p}$-nucleus atoms which may be even more sensitive to off-shell effects.

After analytically continuing our calculational techniques and the Graz interaction model, we were able to find bound and resonant states of baryonium in a number of charge and isospin channels. Some have widths as large as 115 MeV, others have widths as narrow as 16 MeV—and may be observable. We have also found that our extrapolation of the Graz potential to energies far below the scattering region can yield very deeply bound ($|E_R| \geq 300$ MeV) baryonium states with zero width. However, these states appear to be an artifact of the model.

ACKNOWLEDGMENTS

This work was supported in part by the U.S. Department of Energy under Grant No. DE-FG06-86ER40283,A001. We wish to acknowledge the assistance of M. Sagen, and to thank W. Plessas, M. Alberg, A. Stetz, and G. He for helpful conversations.

[1]E. Auld *et al.*, Phys. Lett. **77B**, 454 (1978).

[2]T. P. Gorringe, J. D. Davies, J. Lowe, J. M. Nelson, S. M. Playfer, G. J. Pyle, G. T. A. Squire, C. A. Baker, C. J. Batty, S. A. Clark, A. I. Kilvington, J. Moir, S. Sakamoto, R. E. Welsh, R. G. Winter, and E. W. A. Lingeman, Phys. Lett. **162B**, 71 (1985).

[3]C. A. Baker, C. J. Batty, J. D. Davies, C. W. E. van Eijk, R. Ferreira Marques, R. W. Hollander, D. Langerveld, E. W. A. Lingeman, J. Lowe, J. Moir, J. M. Nelson, W. J. C. Okx, G. J. Pyle, S. Sakamoto, A. Selvarajah, G. T. A. Squier, R.

E. Welsh, R. G. Winter, and A. Zoutendijk in Proceedings of the 8th European Symposium on $N\bar{N}$ Interactions, Thessaloniki, Greece, 1986.

[4]S. Ahmad, C. Amsler, R. Armenteros, E. G. Auld, D. Axen, D. Bailey, S. Barlag, G. A. Beer, J. C. Bizot, M. Caria, M. Comyn, W. Dahme, B. Delcourt, M. Doser, K. D. Duch, K. L. Erdman, F. Feld-Dahme, U. Gastaldi, M. Heel, R. Howard, B. Howard, J. Jeanjean, H. Kalinowsky, F. Kayser, E. Klempt, R. Landau, G. Marshall, H. Nguyen, N. Prevot, L. Robertson, C. Sabev, U. Schaefer, R. Schneider, O. Schreiber, U. Straumann, P. Truoel, B. White, W. R. Wodrich, and M. Ziegler, CERN Report CERN-EP/85-05, 1985.

[5]M. Krell, Phys. Rev. Lett. **26**, 584 (1971); R. Seki, Phys. Rev. C **5**, 1196 (1972); J. H. Koch, M. M. Sternheim, and J. F. Walker, Phys. Rev. Lett. **26**, 1465 (1971).

[6]A. E. Kudryavtsev and V. S. Popos, Pis'ma Zh. Eksp. Teor. Fiz. **29**, 311 (1979) [Sov. Phys.—JETP Lett. **29**, 280 (1979)]; V. S. Popov, A. E. Kudryavtsev, and M. D. Mur, Zh. Eksp. Teor. Fiz. **77**, 1729 (1979) [Sov. Phys.—JETP **50**, 865 (1979)].

[7]C. B. Dover, Brookhaven National Laboratory Report BNL 38288, 1986.

[8]J. M. Richard, M. Lacomb, and R. Vinh Mau, Phys. Lett. **64B**, 121 (1976); M. Lacomb, B. Loiseau, B. Moussallam, and R. Vinh Mau, Phys. Rev. C **29**, 1800 (1984).

[9]M. Lacombe, B. Loiseau, J. M. Richard, R. Vinh Mau, J. Côté, P. Pirè, and R. de Tourreil, Phys. Rev. C **21**, 861 (1984); J. Côtè, M. Lacombe, B. Loiseau, B. Moussallam, and R. Vinh Mau, Phys. Rev. Lett. **48**, 1319 (1982).

[10]W. Buck, C. B. Dover, and J. M. Richard, Ann. Phys. (N.Y.) **121**, 47 (1979); C. B. Dover and J. M. Richard, *ibid.* **121**, 70 (1979); Phys. Rev. C **21**, 1466 (1981).

[11]A. M. Green, and S. Wycech, Nucl. Phys. **A377**, 441 (1982); A. M. Green, J. A. Nishkanen, and S. Wycech, Phys. Lett. **139B**, 15 (1984); A. M. Green, W. Stephen-Rudzka, and S. Wycech, Nucl. Phys. **A399**, 307 (1983).

[12]J. C. H. Van Doremalen, Yu. A. Sionov, and M. Van der Velde, Nucl. Phys. **A340**, 317 (1980).

[13]I. S. Shapiro, Phys. Rep. **35C**, 129 (1978).

[14]F. Myhrer and A. W. Thomas, Phys. Lett. **64B**, 59 (1976); F. Myhrer and A. Gersten, Nuovo Cimento **A37**, 21 (1977).

[15]M. A. Alberg, R. A. Freedman, E. M. Henley, W-Y. P. Hwang, D. Seckel, and L. Wilets, Phys. Rev. D **27**, 536 (1983).

[16]F. Myhrer, International Conference Hadronic Probes and Nuclear Interactions, Phoenix, 1985; R. Tegen, T. Mizutani, and F. Myhrer, University of South Carolina report, 1985.

[17]Y. R. Kwon and F. Tabakin, Phys. Rev. C **18**, 932 (1978).

[18]E. Hernàndez and A. Mondragon, Phys. Rev. C **29**, 722 (1984).

[19]B. Gyarmati, A. T. Kruppa, and Z. Papp, Phys. Rev. C **31**, 2317 (1985).

[20]A general solution for a *single* channel in momentum space as discussed in Ref. 17 is provided by the code BOPIT, D. P. Heddle, Y. R. Kwon, and F. Tabakin, Comput. Phys. Commun. **28**, 109 (1982).

[21]R. H. Landau, Phys. Rev. C **23**, 1324 (1983); **27**, 2191 (1983).

[22]R. H. Landau and B. Cheng, Phys. Rev. C **33**, 734 (1986).

[23]W. Schweiger, J. Haidenbauer, and W. Plessas, Phys. Rev. C **32**, 1261 (1985).

[24]J. Thaler, J. Phys. G **10**, 1037 (1984).

[25]J. M. Richard and M. E. Saino, Phys. Lett. **110B**, 349 (1982).

[26]H. H. Brouwer, J. W. de Maag, and L. P. Kok, Z. Phys. A **318**, 1 (1984).

[27]J. Schnick and R. H. Landau, Phys. Rev. Lett. **58**, 1719 (1987).

[28]J. Côté *et al.*, Phys. Rev. Lett. **48**, 1319 (1982).

[29]We calculate Ref. 23's $\Delta m_{1A} = -300$ MeV to mean $m_B = 788$ MeV $[\Delta M_{1A} = 2(m_B - m_p)]$. Although the "location of the threshold is not so crucial" in Ref. 23's fit to scattering, we find it critical in the location of deep baryonium states.

[30]M. I. Haftel and F. Tabakin, Nucl. Phys. **158**, 1 (1970).

[31]In view of the fact that baryonium states can be deeply bound, and the energy released into annihilation channels can be large, it would be better to use relativistic definitions of energies in the Schrödinger equation or a relativistic wave equation. However, consistency with the input potential (Ref. 23) requires a nonrelativistic formulation.

[32]J. M. Eisenberg and W. Greiner, *Nuclear Theory* (North-Holland, Amsterdam, 1976), Vol. 2, p. 245.

[33]S. Deser, M. L. Goldberger, K. Bauman, and W. Thirring, Phys. Rev. **96**, 774 (1954); T. H. Trueman, Nucl. Phys. **26**, 57 (1961).